Earthquakes and Structures, *Vol. 9, No. 5 (2015) 1029-1044*
DOI: http://dx.doi.org/10.12989/eas.2015.9.5.1029

Pounding analysis of RC bridge considering spatial variability of ground motion

Qiang Han*, Huihui Dong, Xiuli Du and Yulong Zhou

Key Laboratory of Urban Security and Disaster Engineering of Ministry of Education, Beijing University of Technology, Beijing 100124, China
Beijing Collaborative Innovation Center for Metropolitan Transportation, Beijing 100124, China

(Received November 24, 2014, Revised February 20, 2015, Accepted May 8, 2015)

Abstract. To investigate the seismic pounding response of long-span bridges with high-piers under strong ground motions, shaking table tests were performed on a 1/10-scaled bridge model consisting of three continuous spans with rigid frames and one simply-supported span. The seismic pounding responses of this bridge model under different earthquake excitations including the uniform excitation and the traveling wave excitations were experimentally studied. The influence of dampers to the seismic pounding effects at the expansion joints was analyzed through nonlinear dynamic analyses in this research. The seismic pounding effects obtained from numerical analyses of the bridge model are in favorable agreement with the experimental results. Seismic pounding effect of bridge superstructures is dependent on the structural dynamic properties of the adjacent spans and characteristics of ground motions. Moreover, supplemental damping can effectively mitigate pounding effects of the bridge superstructures, and reduce the base shear forces of the bridge piers.

Keywords: seismic pounding; isolation device; traveling wave excitation; shaking table test; nonlinear analysis

1. Introduction

Reinforced concrete (RC) bridges with high-piers are widely used in the mountainous zones with high seismic intensities. Hollow section bridge columns are commonly adopted to the substructures of these bridges, because they can effectively reduce the inertia contribution of the columns to the seismic response of the bridges and offer optimal strength/mass ratios and stiffness/mass ratios to the bridge substructure. The superstructures of these bridges usually consist of continuous rigid frames and multi-span, simply-supported girders with several expansion joints minimizing temperature induced stresses. The reconnaissance reports from recent earthquakes such as Wenchuan earthquake (M8.0, 2008), Yushu earthquake (M7.1, 2010), and Lushan earthquake (M7.0, 2013) in China, have repeatedly demonstrated the seismic vulnerability of existing RC bridges, especially those with hollow section high-piers (Han *et al.* 2009, 2013, 2014). Earthquake-induced pounding between adjacent spans at the expansion joints is one of the major

*Corresponding author, Professor, E-mail: qhan@bjut.edu.cn

Copyright © 2015 Techno-Press, Ltd.
 ISSN: 2092-7614 (Print), 2092-7622 (Online)

causes of the longitudinal unseating of a continuous bridge under strong earthquake excitations and has been studied extensively after Loma Prieta earthquake (M7.0, 1989) in the USA.

Pounding between adjacent spans of the bridge is a very complex phenomenon, which may involve plastic deformations, local concrete crushing and fracture at the contacted locations. Idealizations and assumptions have inevitably been used in the existing theoretical models, among which two modelling techniques have been widely used: the contact approach and the stereo-mechanical approach (Susendar and Reginald 2006). The contact approach includes the linear spring model (Maison and Kasai 1990, 1992), Kelvin model (Jankowski *et al*. 1998, Marhefka and Orin 1999), Hertz model (Jankowski *et al*. 1998, Jankowski 2005), Hertz-damp model (Chauk and Wei 2001), modified Hertz-damp model (Jankowski 2005), and 3D contact friction model (Zhu, 2001). With regard to the pounding effect of bridge superstructures, previous research (Mander *et al*. 1999) showed that the pounding effect between two decks reduces the internal force of bridge piers. However, a large number of studies indicated that the collision effects of the bridge decks significantly increase the seismic response of the bridge decks and bridge piers (e.g., Pantelides and Ma 1998, Jankowski 2002), and the two-pounding amplifies the response of stiff frame but reduces the response of flexible frame (Reginald and Susendar 2002). Some researchers (Anat 2001, Jankowski 2000, Zanardo 2002) pointed out that parameters including the frame stiffness ratios, seismic loading, the widths of expansion joints and the frame yield strength are of great importance in determining the pounding effects in multiple-frame bridges. Moreover, some experiments (Li 2007) have been conducted to investigate the effects of pounding between buildings observed in the field. However, the seismic pounding response of the superstructures in a long span bridge accounting for the spatial variability of ground motion remains uncertain in current research.

To investigate the seismic pounding response of long-span bridges with high-piers under strong ground motions, shaking table tests were performed on a 1/10-scale bridge model consisting of three continuous spans with rigid frames and one simply-supported span in earthquake engineering Laboratory at Beijing University of Technology. The bridge model was built in details including RC hollow section piers, bearings dampers and multi-span simply-supported girders. The bridge model was subjected to strong earthquake ground motion during the shake table tests. Numerical simulations of the tests were also conducted using OpenSees finite element (FE) platform. Kelvin model was adopted in the numerical model to simulate the pounding effects at the expansion joints during earthquakes. The main objectives of this paper are: 1) to predict seismic pounding response of a 1/10 scaled bridge model under different seismic excitations including both the uniform excitation and the asychronized representing the traveling seismic waves; 2) to evaluate the effectiveness of supplemental damping in reducing the seismic pounding effects.

2. Bridge model

The prototype of the high pier bridge (overall length is 160 m) with hollow section consists of three continuous spans with ridge frames (spans length is 35 m, 60 m, and 35 m, respectively) and one span of simply-supported girders (span length is 30 m). Based on the loading capacities, of the shake tables, a 1/10 scaled bridge model was constructed, as shown in Fig. 1.

The detailed configurations of the bridge model are shown in Fig. 2. To satisfy the inertia demand of the superstructure with RC box section, additional masses of approximately 5.5 tons were uniformly distributed on the deck. The cross-sectional height of the first span varies from 0.3

Fig. 1 Elevation view of 1/10-scale bridge model

Table 1 Design parameters of viscous damper

Inner diameter /m	Diameter of piston head/m	Length of piston head/m	Diameter of piston rod/m	Diameter of damping hole/m	Length of damping hole/m	Number of damping hole	Viscosity of viscous liquid/cst
0.05	0.05	0.05	0.028	0.002	0.05	4	100

m to 0.45 m. The height of the cross-section at mid-span of the second span is 0.2 m with a parabola profile along the axial direction of the bridge, as shown in Fig. 2. The height of all RC hollow piers is 3.0 m. The cross-sectional dimension of the rectangular hollow section is 0.4 m by 0.3 m with a wall thickness of 0.1 m.

In order to mitigate pounding response of bridge model, three orifice-type viscous dampers were installed in the last span between the deck and the pier of the bridge model to mitigate pounding response as shown in Fig. 2. The maximum axial force of the viscous damper is approximately 30 kN. Critical parameters of the viscous dampers are listed in Table 1. In addition, a tension-compression sensor was installed on each position of these dampers to monitor the axial force. Laminated rubber bearings with dimensions of 90 mm and 30 mm, were installed on the top of the piers, the total number of rubber layer is nine.

The initial separation distance between two adjacent girders was approximately 6.0 mm as suggested by Chinese code (JTG/T B02-02-2008) for design of highway bridges. A steel tube with a diameter of 50 mm was equipped in the center of the section of the continuous rigid frame bridge, and a steel hemisphere with diameter of 100 mm facing towards the steel pipe was installed at the identical position for the simply-supported bridge. The detailed configurations for the two components are shown in Fig. 2.

3. Analytical modeling of bridge

3.1 Nonlinear elements for bridge

An appropriate nonlinear material model from the material library of the OpenSees program was selected for each component of bridge, as shown in Fig. 2. The superstructure and the cap

beams were assumed to remain elastic during earthquakes and were modeled using elastic beam-column elements. The "Nonlinear-Beam-Column" element available in OpenSees, which is a force-based nonlinear beam-column element and considers the spread of plasticity, was adopted in the numerical simulation for RC columns. Fiber cross section in OpenSees was used for the cross sections of the RC columns. Three types of different constitutive models, confined concrete, unconfined concrete, and longitudinal rebar, were assigned to the fibers in the cross section of the RC columns according to their locations. The properties of the transverse rebar in the column were used to determine the behavior of the confined concrete. Concrete-01 uniaxial material was used for both confined and unconfined concrete in the hollow bridge piers, with the concrete parameters of the hollow piers as listed in Table 2. Steel-02 material model with a symmetric bilinear stress-strain relationship and strain hardening characteristics was utilized to model the longitudinal rebar (F_y=385 N/mm^2, E_0=2.0E5 N/mm^2). The rubber bearing was modeled using bi-linear model, as shown in Fig. 2. Its initial stiffness was calculated using the geometries and material properties of the elastomeric pad and the lead core. The viscous damper of bridge model as shown in Fig. 2 was simplified by Maxwell model (Nicos and Constantinou 1991, Mahendra 2003)

$$k_{eq} d_i = c_{eq} (\dot{d}_j)^{\alpha} \tag{1}$$

Where k_{eq} is equivalent stiffness; c_{eq} is equivalent damping coefficient of Maxwell model.

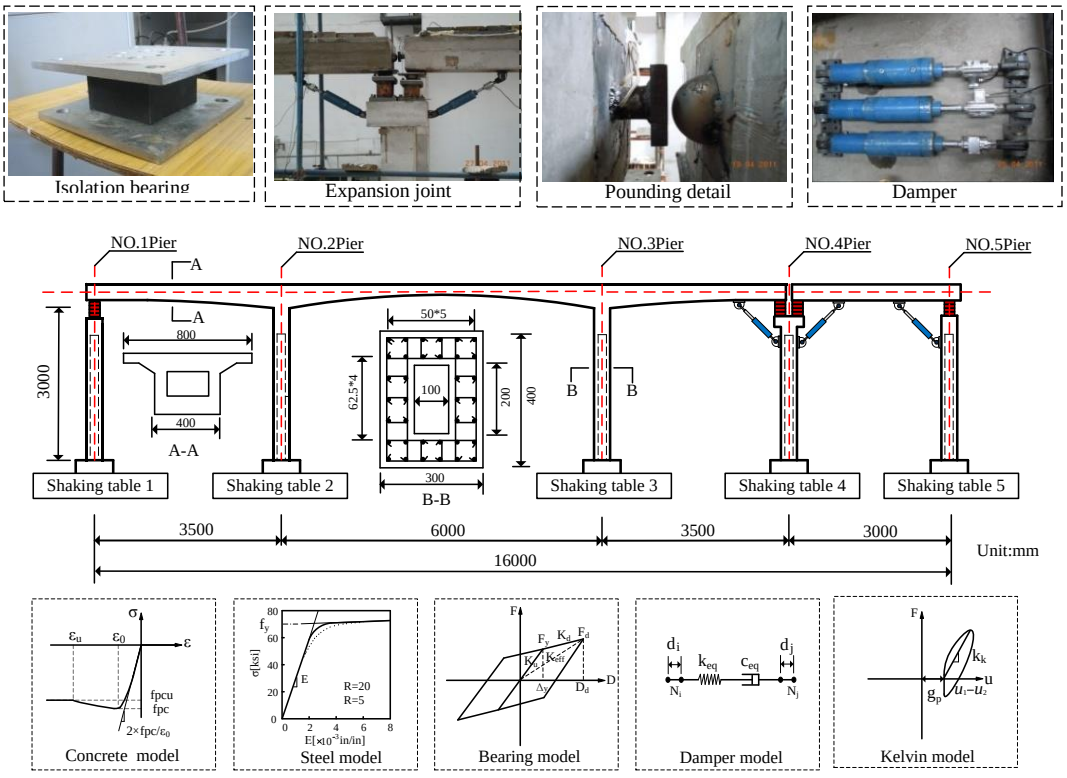

Fig. 2 Analytical model and configuration of bridge

Table 2 Concrete parameters of RC hollow piers

Concrete	$f_c^{'}/MPa$	ε_0	$f_u^{'}/MPa$	ε_u
Unconfined concrete	35.3	0.002	7.1	0.004
Confined concrete	45.9	0.0026	9.18	0.015

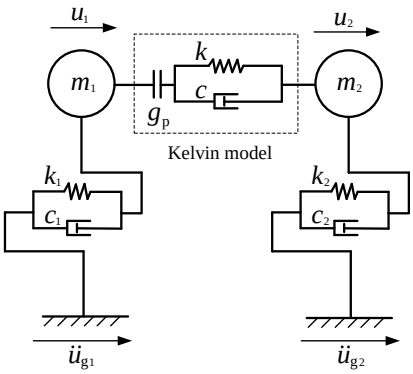

Fig. 3 Simplified pounding model of two adjacent spans

3.2 Pounding model

In order to investigate seismic pounding between adjacent decks, a simplified pounding model with two degrees-of-freedom (DOF) was developed, as shown in Fig. 3. Each adjacent deck was simplified by a single-degree-of-freedom system (SDOF), which is characterized by a mass, m_i, an initial stiffness, k_i and a viscous damping coefficient, c_i. The SDOF system is assumed to behave linear elastically. Using a force-based approach to model the impact, the equation of motion for this two-DOF system subjected to horizontal ground motion $\ddot{u}_g$ can be written as

$$\begin{bmatrix} m_1 & \\ & m_2 \end{bmatrix}\begin{Bmatrix} \ddot{u}_1 \\ \ddot{u}_2 \end{Bmatrix}+\begin{bmatrix} c_1 & \\ & c_2 \end{bmatrix}\begin{Bmatrix} \dot{u}_1 \\ \dot{u}_2 \end{Bmatrix}+\begin{bmatrix} k_1 & \\ & k_2 \end{bmatrix}\begin{Bmatrix} u_1 \\ u_2 \end{Bmatrix}+\begin{Bmatrix} F_c \\ -F_c \end{Bmatrix}=-\begin{bmatrix} m_1 & \\ & m_2 \end{bmatrix}\begin{Bmatrix} \ddot{u}_{g1} \\ \ddot{u}_{g2} \end{Bmatrix} \tag{2}$$

Where $\ddot{u}_i$, $\dot{u}_i$, u_i are the acceleration, the velocity and the displacement relative to the ground, respectively; F_c is the contact force due to pounding.

Pounding is a highly non-linear phenomenon, accompanied with several uncertainties in its mathematical modeling. Previous research results indicated that the system displacement from the stereo-mechanical approach, Kelvin and Hertz damp models are similar for a given coefficient of restitution using different impact methodologies.

The displacements errors by five different contact models of the same system are not more than 12% (Muthukumar and Reginald 2006). Therefore, Kelvin model was used in this study since its parameters are easier to be determined and the energy losses of the two-DOF system during pounding were studied in this paper.

In Kelvin model, a linear spring with stiffness of k_k, is connected in parallel to a dashpot with a damping coefficient of c_k, which accounts for energy dissipation during the impact. The impact force-displacement relation, as shown in Eq. (2), can be calculated as follows

Table 3 Input earthquake ground motion cases

No.	Input waves	PGA (g)	Excitation mode
1	El-Centro wave	0.385/1.1	Uniform excitation/Traveling-wave excitation
2	Wenchuan wave	0.385/1.1	Uniform excitation/Traveling-wave excitation
3	Beijing wave	0.385/1.1	Uniform excitation/Traveling-wave excitation

$$\begin{cases} F_c = K_k(u_1 - u_2 - g_p) + c_k(\dot{u}_1 - \dot{u}_2), u_1 - u_2 - g_p \geq 0 \\ F_c = 0, u_1 - u_2 - g_p < 0 \end{cases} \tag{3}$$

The damping coefficient c_k can be related to the coefficient of restitution, r, by equating the energy losses during impact

$$c_k = 2\varsigma\sqrt{K_k \frac{m_1 m_2}{m_1 + m_2}} \tag{4}$$

$$\varsigma = -\frac{\ln r}{\sqrt{\pi^2 + (\ln r)^2}} \tag{5}$$

Where, m_1 and m_2 are the masses of the colliding bodies, s is the recovery coefficient of collision energy dissipation, which ranges between 0.5 and 0.75 (Khoei 2007). Perfectly elastic collision occurs when r=1.0 and fully plastic collision occurs when r=0. Previous research indicated that for a certain recovery coefficient, the displacements of the above several models are very close to each other (Wang *et al*. 2004, Wang *et al*. 2006, Cole *et al*. 2011). So Kelvin model with a linear spring and a viscous damper was adopted in this paper to simulate the ponding effects.

3.3 Input earthquake ground motion

The experiment was conducted on the multiple shaking tables at the Key Laboratory of Urban Security and Disaster Engineering of Beijing University of Technology, China. Three ground motion records were selected: El-Centro acceleration time-history (Imperial Valley USA, 1940, N-S), Wenchuan acceleration time-history (Wenchuan China, 2008, N-S) and Beijing acceleration time-history (the artificial seismic wave). The peak ground accelerations (PGA) are 0.385 g and 1.1 g corresponding to frequently and rarely occurred earthquakes which were determined based on the similarity ratio and the capacity of shaking table. Input earthquake ground motions used in the shaking table tests were presented in Table 3. Fig. 4 illustrates the full-scale input acceleration time-histories for both shake-table test and numerical simulations. The excitation was applied at the bases of the piers in the longitudinal direction of the bridge. To investigate the traveling wave effect, time of inputting motions for each column was varied by a time-lag, calculated by assuming a constant propagation velocity of 100m/s. Therefore, time lags of 1 s, 2.5 s, 3.5 s and 4.5 s were introduced to the input earthquake excitations imposed at the bottoms of Pier 2 to Pier 5, respectively.

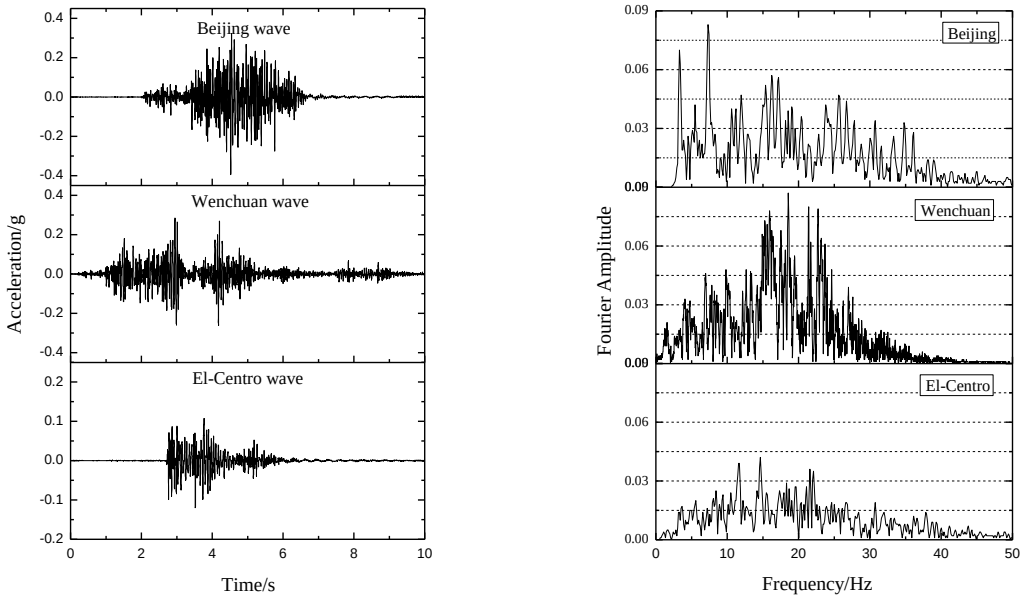

Fig. 4 Seismic wave for input in the experiment and Fourier spectrum

4. Numerical analysis

4.1 Pounding effects for seismic response of bridge

In order to investigate the influence of the pounding effect on the seismic response of the bridge under strong ground motions, numerical models with and without pounding element were built in OpenSees. Nonlinear time-history analyses were performed on both numerical models and the results were compared and discussed in the following section.

Table 4 shows the peak displacements at the top of the piers with and without pounding effects. It can be observed that when pounding occurs, the peak displacement at the top of Pier 2 decreases from 10.2 mm to 9.6 mm under El-Centro earthquake motion, and it decreases from 19.460 mm to14.880mm under Beijing earthquake motion; while the displacement at the top of Pier 2 increases from 32.641 mm to 46.279 mm, which is 1.42 times of the displacement without pounding for Wenchuan earthquake motion. Pounding has little effect on side piers of the bridge model.

Fig. 5 shows the seismic response of the bridge with and without pounding. Fig. 5 indicated that when pounding occurs, the moment at the bottom of Pier 2 decreases for both El-Centro and Beijing earthquake motions. Moreover, pounding also reduces the curvature at the bottom of Pier 2 from 4.6E-6 to 3.4E-6 for Beijing earthquake motion. The moment at bottom of Pier 2 becomes 2.27 times of the moment without pounding, and the curvature at the bottom of Pier 2 becomes 1.2 times of the curvature without pounding for Wenchuan earthquake motion. For El-Centro wave (0.385 g), the relative displacement increase from 10 mm to 18 mm with pounding; while for Wenchuan wave (1.1 g), it decrease from 35 mm to 25 mm. Moreover, because of the small inherent damping in the bridge, the relative displacements between two adjacent decks attenuated slowly after all the earthquake motions. When pounding occurs, the pounding effect may increase

or decrease the relative displacement between adjacent decks depending on the characteristics of the input excitations.

It can be concluded that the pounding effect for seismic response of bridge between adjacent decks is apparent. Impact effect may limit the relative displacement between adjacent decks, and energy dissipation, while the pounding effect of bridge model may also increase seismic response.

Table 4 Peak displacements at the top of piers with pounding and without pounding

Input wave	Conditions	Pier 1 (mm)	Pier 2 (mm)	Pier 3 (mm)	Pier 4 (mm)	Pier 5 (mm)
El-Centro (0.385 g)	With pounding	2.462	10.172	10.178	2.025	1.99
	No pounding	2.462	9.561	9.560	2.482	2.842
Beijing (0.385 g)	With pounding	2.291	19.460	19.461	3.518	2.783
	No pounding	2.864	14.880	14.881	4.621	4.364
Wenchuan (0.385 g)	With pounding	2.846	7.491	7.492	3.496	3.213
	No pounding	2.858	8.817	8.816	3.347	3.291
El-Centro (1.1 g)	With pounding	12.630	38.405	38.406	12.132	11.150
	No pounding	12.599	34.601	34.602	13.945	12.246
Beijing (1.1 g)	With pounding	16.011	41.075	41.076	17.203	17.552
	No pounding	18.485	38.876	38.877	16.825	19.374
Wenchuan (1.1 g)	With pounding	12.919	32.641	32.641	13.143	11.507
	No pounding	14.977	46.279	46.279	18.266	15.390

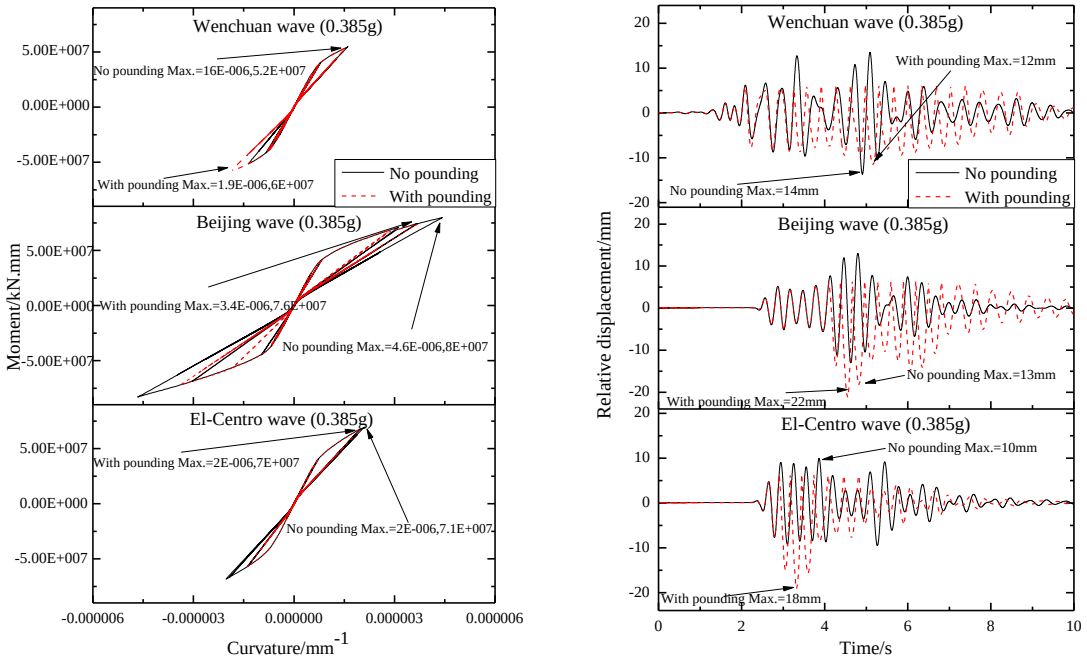

(a) Moment vs curvature hysteresis at bottom of pier 2 (b) Relative displacement between two decks

Fig. 5 Seismic response of the bridge with pounding and without pounding (PGA=0.35 g and PGA=1.1 g)

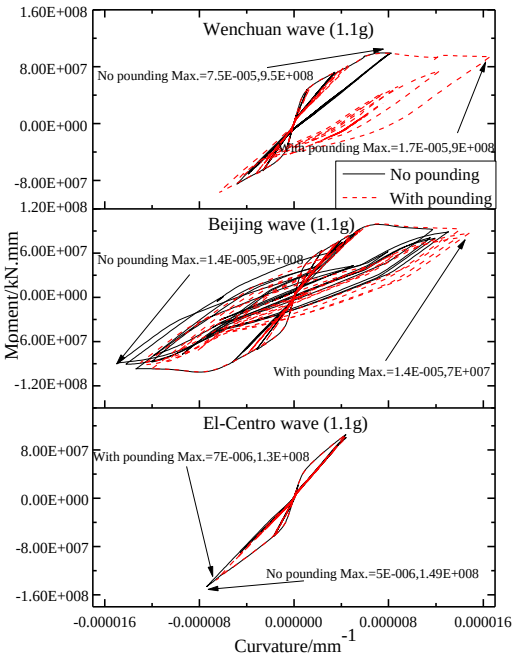

(c) Moment vs curvature hysteresis at bottom of pier 2

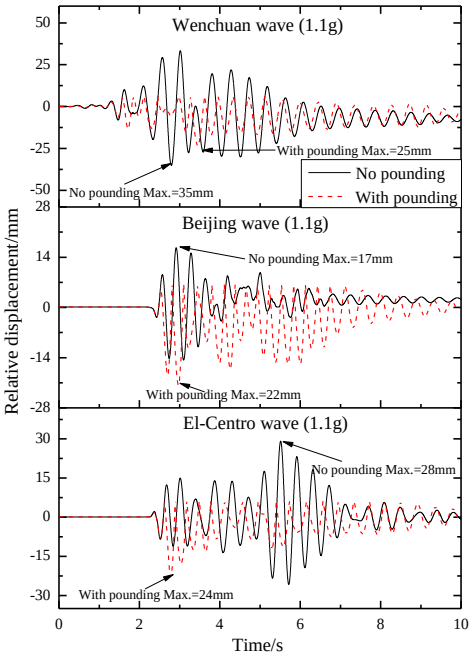

(d) Relative displacement between two decks

Fig. 5 Continued

4.2 Influence of traveling wave excitation on pounding effect

In order to investigate the influence of traveling wave excitation to the pounding response of bridge model, nonlinear time-history analyses were performed on the same the bridge model with pounding element using both uniform excitation and traveling wave excitation.

Table 5 shows the peak displacements at the top of the piers under uniform excitation and traveling wave excitation. Compared with the results using uniform excitation, the peak displacements of the top of Pier 2 and 3 are less than those using traveling wave excitation, which reduce from 14.880mm to 9.083mm, (reduce by 39%) for Beijing earthquake motion; while for El-Centro and Wenchuan earthquake motion, the peak displacements at the top of all the piers are all larger, and the peak displacement at the top of Pier 2 increases from 8.817 mm to 17.171 mm

Table 5 Displacements at top of piers for uniform excitation and traveling wave excitation/mm (PGA=1.1 g)

Input wave	Conditions	Pier 1	Pier 2	Pier 3	Pier 4	Pier 5
El-Centro (1.1 g)	Uniform excitation	11.330	10.215	10.215	10.229	11.866
	Traveling-wave excitation	2.462	9.561	9.560	2.482	2.842
Beijing (1.1 g)	Uniform excitation	8.688	9.083	9.083	7.825	9.257
	Traveling-wave excitation	2.864	14.880	14.881	4.621	4.364
Wenchuan (1.1 g)	Uniform excitation	13.223	17.171	17.171	11.675	14.337
	Traveling-wave excitation	2.858	8.817	8.816	3.347	3.291

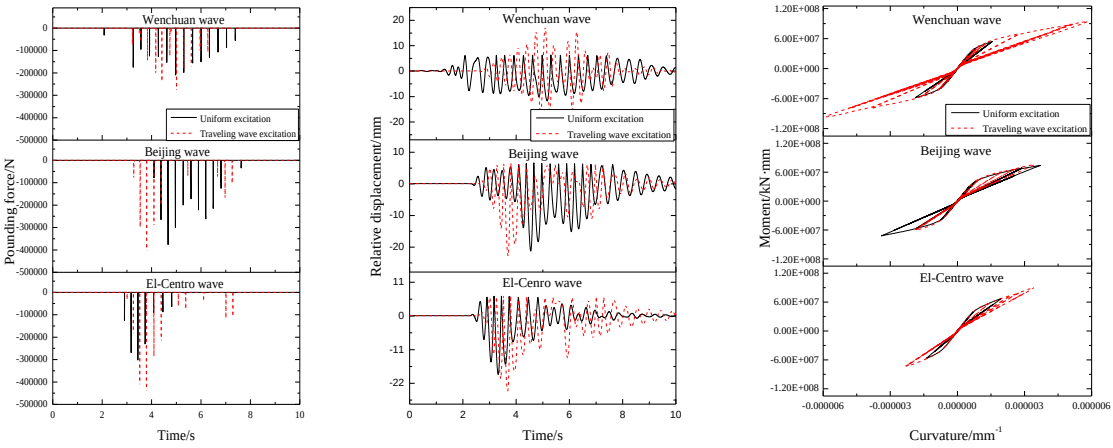

(a)Pounding force (b)Moment vs curvature hysteresis at bottom of pier2 (c)Relative displacement between two decks

Fig. 6 Seismic response of bridge models for uniform excitation and traveling wave excitation (PGA=1.1 g)

for Wenchuan earthquake motion. Moreover, traveling wave excitation has more significant influence to the piers at two ends of the bridge model compared to that of uniform excitation. The displacement at the top of Pier 1 increase from 2.858 mm to 13.880 mm (4.8 times) for El-Centro earthquake motion.

Fig. 6 shows the seismic response of the bridge under uniform excitation and traveling wave excitation. The pounding effects of bridge model increased or decreased under traveling wave excitation. Under traveling wave excitation, less pounding times and smaller pounding forces between two adjacent girders can be observed from the analytical results. The pounding times reduce by approximately 30% and the curvature at bottom of Pier 2 reduces from 3.8 E-6 to 3.5 E-6 for Beijing earthquake motion. However, for Wenchuan earthquake motion, the pounding force increase by 25%, and the pounding times are 14 times under traveling wave excitation, which is twice more than that of the case under uniform excitation. In addition, the curvature at the bottom of Pier 2 increases from 1.9 E-6 to 5.9 E-6, and the moment increases from 5.83E+10 to 9.67E+10. Meanwhile, the relative displacement is attenuated slowly under traveling wave excitation, due to the small inherent damping in the bridge.

Overall, it can be addressed that the traveling wave excitation has significant influence on seismic pounding responses of bridge superstructures. However, the influencing mechanism is very complicated and influencing results are complex and indeterminate. The phase difference of earthquake ground motion is formed by traveling wave excitation which lead the seismic response of structure overlaps or removes, so the pounding effect will be intensified or weakened. Moreover, the effects of the traveling wave excitation on the seismic ponding response of the bridge is highly dependent on the bridge structure itself and other circumstances, such as wave type. Traveling wave excitation may increase or decrease seismic pounding response of bridge superstructures compared to uniform excitation due to superposition of earthquake motion.

4.3 Pounding effect with damper

In order to investigate the influence of supplemental damping to the pounding response of the

bridge model under strong ground motions, numerical bridge models with and without additional dampers were built in OpenSees.

Table 6 lists the peak displacements of the top of the piers with and without dampers. Under severe earthquakes (PGA=1.1 g), the displacement at the top of Pier 2 decreases from 46.279 mm to 36.715 mm for Wenchuan earthquake motion after the application of the dampers. The displacement at top of Pier 4 decreases by 49.6% under El-Centro earthquake motion. The dampers effectively reduce the seismic response of the bridges under severe earthquakes. The seismic responses of every part of bridge model tend to coordination due to dampers increasing stiffness of joint parts and affecting the whole performance of bridge. While the displacement at

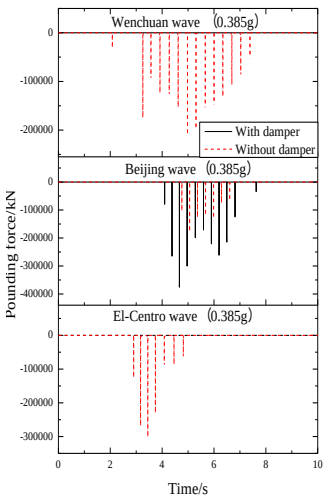

(a) Pounding force

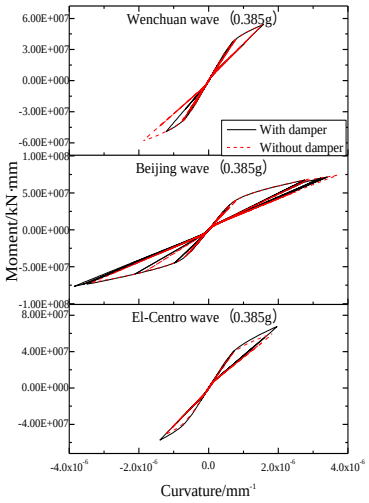

(b) Moment vs curvature hysteresis at bottom of pier2

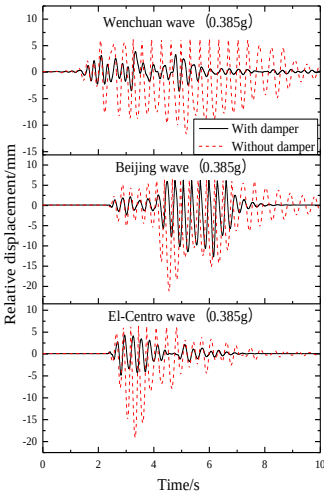

(c) Relative displacement between two deck

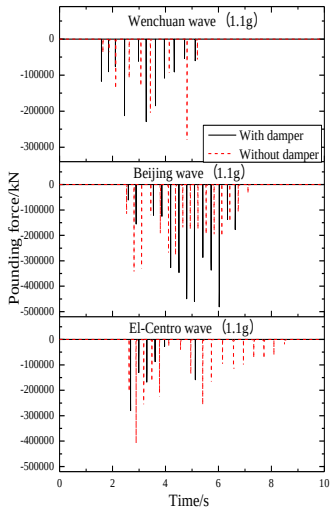

(d) Pounding force

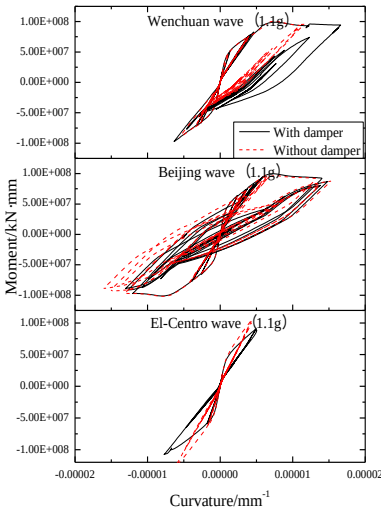

(e) Moment vs curvature hysteresis at bottom of pier2

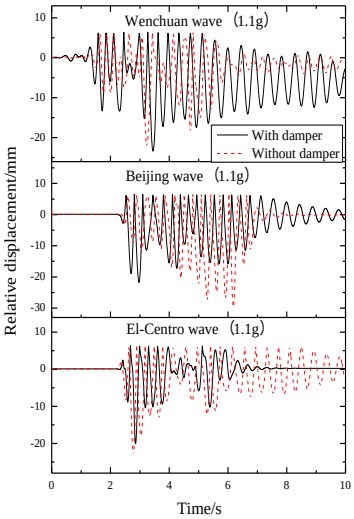

(f) Relative displacement between two decks

Fig. 7 The seismic response of bridge models with and without damper (PGA=0.385 g and PGA=1.1 g)

Table 6 Displacements at top of piers with and without damper/mm

Input wave	Conditions	Pier 1	Pier 2	Pier 3	Pier 4	Pier 5
El-Centro (0.385 g)	With damper	2.419	8.593	8.594	2.431	2.623
	Without damper	2.462	9.561	9.560	2.482	2.842
Beijing (0.385 g)	With damper	3.364	15.869	15.869	7.468	3.614
	Without damper	2.864	14.880	14.881	4.621	4.364
Wenchuan (0.385 g)	With damper	2.826	7.394	7.394	3.031	2.217
	Without damper	2.858	8.817	8.816	3.347	3.291
El-Centro (1.1 g)	With damper	12.599	32.289	32.289	13.945	12.246
	Without damper	13.267	34.601	34.602	20.862	15.321
Beijing (1.1 g)	With damper	18.485	38.876	38.877	16.825	19.374
	Without damper	20.107	43.278	43.279	34.684	27.014
Wenchuan (1.1 g)	With damper	14.869	36.715	36.715	16.648	9.614
	Without damper	14.977	46.279	46.279	18.266	15.390

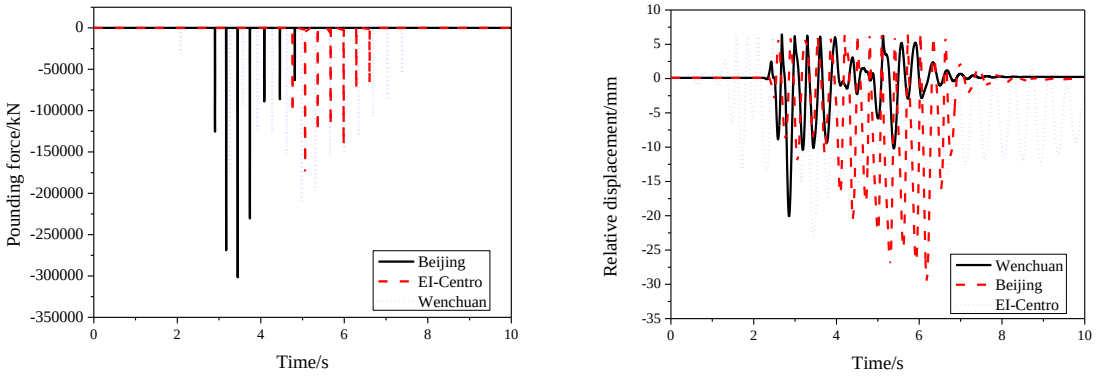

Fig 8 The seismic response of bridge models under various earthquake ground motion

the top of Pier 4 increase from 4.621 mm to 7.468 mm for Beijing earthquake motion under moderate earthquakes (PGA=0.385 g).

The seismic response of the bridge with and without dampers is presented in Fig. 7. No pounding occurred for the bridge model subjected to El-Centro and Wenchuan earthquake motion when dampers were provided, and the peak moment at the bottom and the peak relative displacement at the top of Pier 2 are significantly reduced. The peak relative displacement decreases from 12.2 mm to 4 mm for Wenchuan earthquake motion. Meanwhile, the time-histories of the relative displacement decreased much faster for the case with dampers under all three earthquake motions.

It is effective to provide supplemental damping for the mitigation of pounding effects between bridge decks. The base shear forces in the bridge piers and the pounding forces carried by the superstructure can be satisfactorily reduced after the installation of viscous dampers in the given locations. The effectiveness of dampers is related to the input excitations and the characteristics of the bridge structure.

Table 7 Displacements at top of piers under various earthquake ground motion/ mm

Input wave	Pier 1	Pier 2	Pier 3	Pier 4	Pier 5
El-Centro(0.385g)	2.462	9.561	9.560	2.482	2.842
Beijing(0.385g)	2.864	14.880	14.881	4.621	4.364
Wenchuan(0.385g)	2.858	8.817	8.816	3.347	3.291
El-Centro(1.1g)	13.267	34.601	34.602	20.862	15.321
Beijing(1.1g)	20.107	43.278	43.279	34.684	27.014
Wenchuan(1.1g)	14.977	46.279	46.279	18.266	15.390

Table 8 Comparison of the natural vibration period measured values with finite element calculation value

Vibration mode	1	2	3	4	5	6	7	8
Direction	Transverse	Transverse	Longitudinal	Vertical	Transverse	Longitudinal	Vertical	Transverse
Measured value (s)	0.246	0.236	0.174	0.135	0.121	0.089	0.057	0.030
Calculated value (s)	0.242	0.235	0.157	0.125	0.092	0.058	0.043	0.032
Error (%)	-1.6	0.4	-9.8	-7.4	-23.9	-34.8	-24.5	6.7

4.4 Influence of seismic spectra characteristics on pounding effect

As shown in Fig. 8 and Table 7, seismic responses of the bridge model under Beijing earthquake including peak accelerations, relative displacement and tube strains is the largest. The reason is that the natural period of the bridge model is 0.246 s using the results of the white noise excitations. The Fourier spectra of the three earthquakes are shown in Fig. 4. It is clearly evident that the natural period of the bridge model is close to the predominant period (0.15 s-0.4 s) of the Beijing earthquake. Namely, the dominant frequency of Beijing earthquake covers the natural frequency of the bridge model.

The maximum relative displacements between adjacent girders and the tube strains under various earthquake excitations are shown in Table 7. Evidently, the pounding effects of the bridge model are different under various earthquake motions, which are closely related to spectra characteristics of the ground motion. When the dominant frequency of the earthquake motion covers the basic frequency of bridge structures, seismic pounding responses of the bridge structures will increase significantly.

In order to avoid the unfavorable earthquake responses, adopting isolation and dissipation technologies, such as isolation bearing and additional damper, have the ability to reduce the basic frequency of the structural vibration and dissipate the seismic energy input.

5. Comparison with simulated results and test data of seismic response

The white noise was used to determine the dynamic characteristic of the bridge model. Table 8 compares the natural vibration periods measured from the tests to those from finite element analyses. The results derived from numerical simulations are in good agreement with the experimental data.

Fig. 9 and Fig. 10 compares the acceleration time-histories recorded during the shake-table tests at three critical locations on the bridges to those obtained from the numerical analyses, with the input of three different ground motions. Table 9 compares the peak relative displacements between adjacent decks of experimental and numerical results. It can be seen that there is approximately 10%-20% deviations in the peak acceleration and the peak relative displacement between the simulation and experiment results. This is primarily attributed to the fact that the specimens have different levels of damage under severe earthquakes, while no damage or pinching effects are considered in the simulation. Generally, seismic pounding effects captured by the numerical model are in good agreement with the shake-table test results. Therefore, Kelvin model can be used to simulate the pounding effect between adjacent spans of long span bridges under strong ground motions.

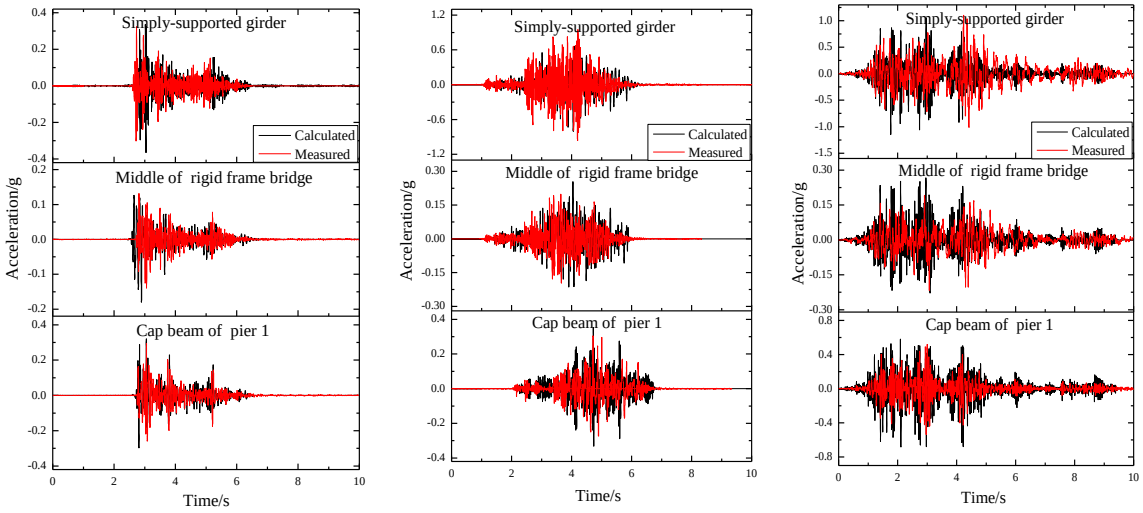

(a)El-Centro wave (b)Beijing wave (c)Wenchuan wave

Fig. 9 Accelerated history comparison of measured and Calculated (PGA=0.385 g)

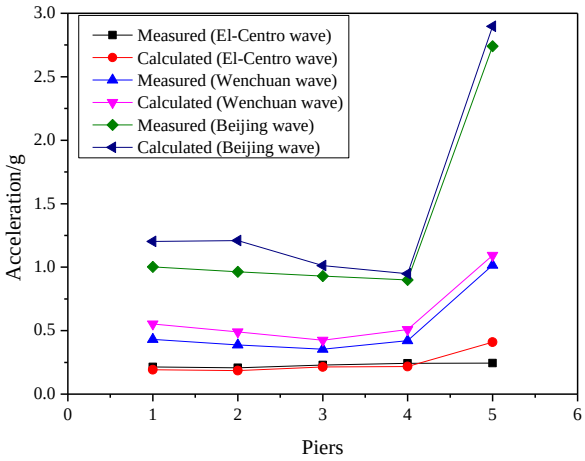

Fig. 10 Comparison of peak acceleration at top of the piers (PGA=1.1 g)

Table 9 Comparison of relative displacement between adjacent decks/mm (PGA=1.1 g)

Condition	LRB						LRB+damper					
	Uniform excitation			Traveling wave excitation			Uniform excitation			Traveling wave excitation		
	El	Wen chuan	Bei jing	El	Wen chuan	Bei jing	El	Wen chuan	Bei jing	El	Wen chuan	Bei jing
Measured	5.3	5.3	7.3	6.5	11.0	9.3	3.6	5.5	5.7	4.3	10.3	9.1
Calculated	4.7	6.0	8.0	6.0	11.7	8.0	4.3	6.1	4.9	5.2	11.2	8.0

6. Conclusions

Multiple shaking table tests of a 1/10-scale bridge model with three continuous rigid frame spans and one simply-supported-girder span were carried out to investigate the seismic pounding response of long-span bridges with high-pier under both uniform and non-uniform earthquake excitations. The pounding response of the bridge model was simulated using OpenSees platform based on a detailed nonlinear model for each component of the bridge model. Based on the numerical and experimental results, the following conclusions can be drawn:

• Kelvin model can accurately capture the pounding effect at the expansion joints. The seismic response of bridges can be either amplified or reduced by the pounding effects depending on the input earthquake excitation.

• The traveling wave effect has significant influence to the seismic pounding response of elevated bridges. Seismic pounding effect of the superstructures under traveling wave excitation may either increase or decrease depending on the characteristics of the bridge and the input motions. The peak pounding force is likely to be underestimated if traveling wave effect is ignored, and it is crucial from the seismic design point of view.

• Supplemental damping can effectively mitigate the pounding effect between bridge superstructures. The effectiveness of the additional dampers in mitigating the seismic damage to the bridges is closely related to the spectral characteristics of the seismic waves and the dynamic properties of the bridge structures. Therefore, it is necessary to optimize parameters of viscous dampers as passive dissipation devices for bridge structures.

Acknowledgements

This research is jointly funded by the National Natural Science Foundation of China (Grants No.51421005 and No.51178008), the research project of Beijing Municipal Commission of Education (Grant No.KZ201410005011), and Program for Changjiang Scholars and Innovative Research Team in University (Grant No. IRT13044). Their supports are gratefully acknowledged.

References

Chauk, T. and Wei, X.X. (2001), "Pounding of structures modeled as non-linear impacts of two oscillators", *Earthq. Eng. Struct. Dyn.*, **30**(5), 633-651.

Cole, G., Dhakal, R., Carr, A. and Bull, D. (2011), "An investigation of the effects of mass distribution on

pounding structures", *Earthq. Eng. Struct. Dyn.*, **40**(6), 641-659.
Han, Q., Du, X., Liu, J., Li, Z., Li, L. and Zhao, J. (2009), "Seismic damage of highway bridges during the 2008 Wenchuan earthquake", *Earthq. Eng. Eng. Vib*., **8**(2), 263-273.
Han, Q., Du, X.L., Zhou, Y.H. and Lee, G.C. (2013), "Experimental study of hollow rectangular bridge column performance under vertical and cyclically bilateral loads", *Earthq. Eng. Eng. Vib*., **12**(3), 433-445.
Han, Q., Zhou, Y., Du, X., Huang, C. and Lee, G.C. (2014), "Experimental and numerical studies on seismic performance of hollow RC bridge columns", *Earthq. Struct*., **7**(3), 251-269.
Jankowski, R., Wilde, K. and Fujino, Y. (1998), "Pounding of superstructure segments is isolated elevated bridge during earthquakes", *Earthq. Eng. Struct. Dyn*., **27**(5), 487-502.
Jankowski, R. (2005), "Non-linear viscoelastic modelling of earthquake-induced structural pounding", *Earthq. Eng. Struct. Dyn.*, **34**(6), 595-611.
Jankowski, R., Wilde, K. and Fujino, Y. (2002), "Pounding of superstructure segments in isolated elevated bridge during earthquake", *Earthq. Eng. Struct. Dyn*., **27**(5), 487-502.
Jankowski, R., Wilde, K. and Fujino, Y. (2000), "Reduction of pounding effects in elevated bridges during earthquakes", *Earthq. Eng. Struct. Dyn.*, **29**(2), 195-212.
Khoei, A.R., DorMohammadi, H. and Azami, A.R. (2007), "A three-invariant cap plasticity model with kinematic hardening rule for powder materials", *J. Mater. Proc. Technol.*, **187**, 680-684.
Li, Z.X., Zhang, Y. and Yue, F.Q. (2007), "Shaking table test on pounding responses of simply supported isolated bridges under earthquake excitation", *Earthq. Eng. Eng. Dyn*., **27**(2), 152-157.
Maison, B.F. and Kasai, K. (1990), "Analysis for type of structural pounding", *J. Struct. Eng.*, **116**(4), 957-977.
Maison, B.F. and Kasai, K. (1992), "Dynamics of pounding when two buildings collide", *Earthq. Eng. Struct. Dyn*., **21**(9), 771-786.
Marhefka, D.W. and Orin, D.E. (1999), "A compliant contact model with nonlinear damping for simulation of robotic systems", *IEEE Transactions on Systems, Man, and Cybernetics-Part A: Systems and Humans*, **29**(6), 566-572.
Mahendra, P.S., Navin, P.V. and Luis, M.M. (2003), "Seismic analysis and design with maxwell dampers", *J. Eng. Mech.*, **129**(3), 273-282.
Mander, J.B., Priestley, M.J.N. and Park, R. (1988), "Theoretical stress-strain model for confined concrete", *J. Struct. Eng.*, **114**(8), 1804-1826.
Muthukumar, S. and Reginald, D. (2006), "A Hertz contact model with non-linear damping for pounding simulation", *Earthq. Eng. Struct. Dyn.*, **35**(7), 811-828.
Nicos, M. and Constantinou, M.C. (1991), "Fractional-derivative maxwell model for viscous dampers", *J. Struct. Eng.*, **117**(9), 2708-2724.
Pantelides, P.C. and Ma, X. (1998), "Linear and nonlinear pounding of structural systems", *Comput. Struct.*, **66**(1), 79-92.
Reginald, D. and Susendar, M. (2002), "Effect of pounding and restrainers on seismic response of multiple-frame bridges", *J. Struct. Eng.*, **128**(7), 860-869.
Ruangrassamee, A. and Kawashima, K. (2001), "Relative displacement response spectra with pounding effect", *Earthq. Eng. Struct. Dyn*., **30**(10), 1511-1538.
Wang, D.S., Feng, Q.M. and Wang, G.X. (2004), "Analysis model of pounding between adjacent bridge girders during earthquakes based on collinear impact between rods", *Eng. Mech*., **21**(2), 157-166.
Wang, J.W., Li, J.Z. and Fan, L.C. (2006), "Effect of pounding at expansion joints on seismic response of irregular girder bridges", *China Civ. Eng. J.*, **39**, 54-59.
Zanardo, G., Hao, H. and Modena, C. (2002), "Seismic response of multi-span simply supported bridges to a spatially varying earthquake ground motion", *Earthq. Eng. Struct. Dyn.*, **31**(6), 1325-1345.
Zhu, P. (2001), "Seismic analysis serviceability evaluation of elevated bridge based on 3D modeling with pounding effects of girders", The University of Tokyo, Tokyo, Japan.